Journal of Petroleum Research and Studies

Open Access
Vol. 14, No. 4, December 2024, pp. 111-128

P- ISSN: 2220-5381
E- ISSN: 2710-1096

DOI: http://doi.org/10.52716/jprs.v14i4.885

Corrosion Mitigation and Cathodic Protection Design for Wet Oil Processing at Qubbat Baba: A Modeling and Simulation Approach using MATLAB Simulink

Qays M. Ammouri*, Hayder M. Majeed, Mays M. Abdulkareem, Dhuha A. Abdulaaima, Buthaina K. Ibraheem, Huda Q. Jabur

Petroleum Research and Development Center, Iraqi Ministry of Oil, Baghdad, Iraq.
*Corresponding Author E-mail: qaysammouri@gmail.com

Received 28/12/2023, Revised 20/03/2024, Accepted 24/03/2024, Published 22/12/2024

Abstract

Oil produced from Qubbat Baba in the Kirkuk oil field -North Oil Company (NOC) requires pre-treatment at the refinery due to water, mineral salts, and sediments. The water contains soluble mineral salts like sodium, calcium, and magnesium chlorides. Failure to treat the crude oil can result in operational problems, such as equipment scaling, corrosion, fouling, and catalyst poisoning in the hydrotreating unit. The study focuses on corrosion in wet oil treatment equipment especially crude oil horizontal separators (process vessels). Corrosion in the internal chamber resulted from two factors: firstly, scale deposition occurred on the surface of Galvalume (GAIII) anodes (passivation phenomenon) during oil-water separation at elevated temperatures (60°C). Secondly, the existing cathodic protection system was inadequate for the crude oil's specifications and the current field's operating conditions for separators. The XRD and XRF chemical analysis revealed that a significant portion of these deposits consisted of Al_2O_3 and ZnO. Based on the provided reasons, the researchers suggested a new design for the Sacrificial Anode Cathodic Protection system (SACP) using MATLAB Simulink software.

Keywords: Kirkuk oil field, cathodic protection, XRD, XRF, SACP, MATLAB Simulink.

تقليل التآكل وتصميم الحماية الكاثودية لمحطة معالجة النفط الرطب / قبة بابا: نمذجة ومحاكاة باستخدام برنامج MATLAB Simulink

الخلاصة:

يتطلب النفط المنتج من قبة بابا في حقل نفط كركوك - شركة نفط الشمال (NOC) معالجة مسبقة في المصفى بسبب احتوائه على الماء والأملاح المعدنية مثل كلوريدات الصوديوم والكالسيوم والمغنيسيوم والرواسب، حيث يؤدي عدم معالجة النفط الخام إلى مشكلات تشغيلية مثل ترسب الرواسب على المعدات، والتآكل، والتلوث، وتسمم المحفزات في وحدة المعالجة الهيدروجينية. تركز الدراسة على التآكل في معدات معالجة النفط الرطب، وخاصة العازلات الأفقية للنفط الخام. ان التآكل في العازلات الافقية يعود الى سببين: الاول بسبب ترسب نواتج التآكل على سطح انودات الجالفالوم GAIII (بسبب ظاهرة

Open Access
Vol. 14, No. 4, December 2024, pp. 111-128
P- ISSN: 2220-5381
E- ISSN: 2710-1096

التخميل) اثناء عملية فصل النفط عن الماء وخصوصا عند ارتفاع درجة الحرارة الى 60 درجة مئوية. ثانيًا، ان نظام الحماية الكاثودية الحالي لايلائم مواصفات النفط الخام وظروف التشغيل الحقلية في العازلات. وضحت تحاليل XRF الكيميائية أن جزءًا كبيرًا من هذه الرواسب يتكون من أوكسيد الألومنيوم (Al_2O_3) وأوكسيد الزنك (ZnO) بناءً على هذه الأسباب، اقترح الباحثون تصميمًا جديدًا لنظام الحماية الكاثودية بالأقطاب المضحية (SACP) باستخدام برنامج MATLAB Simulink.

1. Introduction:

1.1 Corrosion in dehydrators and desalters:

Dehydrators and desalters are specialized equipment used to remove water and salt from crude oil before further processing. Corrosion is a significant concern in the petroleum industry due to the corrosive nature of the substances they handle, such as crude oil, water, and salt. This issue can lead to equipment damage, reduced efficiency, production disruptions, and safety hazards [1] [2] [3] [4] [5] [6].

Corrosion in these units can be attributed to several factors:

a. Chemical Composition: Crude oil often contains impurities like hydrogen sulfide (H_2S) and sulfur compounds that can accelerate corrosion.
b. Water and Salt Content: The presence of water and dissolved salts in crude oil can create a corrosive environment, especially in the presence of oxygen.
c. Temperature and Pressure: Operating conditions, including temperature and pressure, can influence the corrosion rate.
d. Acidic Components: Some components in crude oil can create acidic conditions that promote corrosion.

1.2 Key points to Corrosion Mitigation

- **Materials Selection and Compatibility**: Choosing corrosion-resistant materials for the construction of dehydrators and desalters is crucial. Common materials used include carbon steel, stainless steel, corrosion-resistant alloys (CRAs), and specialized coatings that provide a protective barrier against corrosive substances. It's also important to consider the compatibility of materials used in the construction of these units with the specific crude oil being processed.
- **Chemical Inhibition**: The use of corrosion inhibitors can help mitigate corrosion in dehydrators and desalters. They are added to protect equipment surfaces by forming a protective film.

Open Access
Vol. 14, No. 4, December 2024, pp. 111-128
P- ISSN: 2220-5381
E- ISSN: 2710-1096

- **Cathodic protection**: Implementing sacrificial anodes as a form of cathodic protection can be an effective strategy to mitigate corrosion issues in dehydrators and desalters in the petroleum industry.
- **Process Optimization**: Controlling operating conditions (temperature, pressure, and flow rates) can help reduce the likelihood of corrosion. Proper separation of water and salt from the crude oil is critical to minimize the corrosive effects of these impurities.

1.3 Sacrificial Anodes Cathodic Protection, SACP [7] [8] [9]:

SACP is a corrosion control technique used to protect metal structures, such as pipelines, tanks, and marine vessels, from corrosion. It involves the use of sacrificial anodes made of a more reactive metal, which corrodes sacrificially in place of the protected metal structure. Here's how to apply sacrificial anodes for cathodic protection:

1. **Anode Selection:** Choose the appropriate sacrificial anodes based on the specific conditions of Equipments. Common materials for sacrificial anodes include zinc, aluminum, and magnesium, each with its own level of reactivity. The choice of material depends on the corrosiveness of the environment, operating temperature, and the type of corrosion.
2. **Anode Installation**: Installation of sacrificial anodes in strategic locations in the equipment where corrosion is most likely to occur. It is necessity to ensure good electrical contact between the anodes and the equipment's metal surface through cables or welding …etc.
3. **Monitoring and Inspection**: Regularly monitor the condition of the sacrificial anodes and the protected equipment. Inspection intervals should be determined based on the rate of anode consumption.
4. **Replacement**: When sacrificial anodes have corroded sufficiently, it's essential to replace them with new ones before they are completely consumed to ensure continuous protection.

1.4 SACP Design [8] [10] [11] [12]:

1.4.1 SACP Design Steps:

Designing a SACP system involves the following key steps:

- Identify the metal structure (pipeline, storage tank, offshore platforms…etc.) requiring

Open Access
Vol. 14, No. 4, December 2024, pp. 111-128
P- ISSN: 2220-5381
E- ISSN: 2710-1096

protection from corrosion.

- Assess the corrosion severity in the environment (soil, sea water, industrial).
- Select a suitable anode material (e.g., zinc, aluminum, magnesium).
- Calculate the required anode mass based on surface area and corrosion rate.
- Determine the optimal placement and distribution of anodes on the structure.
- Calculate anode spacing and quantity for even protection.
- Select appropriate mounting hardware (brackets, clamps, or welding) and design electrical connections (low resistance and good electrical contact).
- Establish a monitoring and maintenance plan for regular inspections and anode replacement.
- Install anodes on the structure with correct connections.
- Keep detailed records of system performance and compliance with regulations.

1.4.2 Design equations: As explained below, Table (1) depicts the design equations for SACP system.

Table (1) Design equations for SACP system for dehydrator and desalter [1, 9, 13, 14, 15]

Parameters,	Unit	Equation
h	m	$h=L_W*D_i$
B	---	$B=\sqrt{1+12\,(\frac{h}{D_i}-0.5)^2}$
Ɛ		*it equals 0.866 for semi-ellipsoidal head*
A_{SEh}	m^2	$A_{SEh},=\frac{\pi D_i^2}{8}(\left(\frac{h}{D_i}-0.5\right)B+1+\frac{1}{4_\varepsilon}\ln(\frac{4\varepsilon\left(\frac{h}{D_i}-0.5\right)+B}{2-\sqrt{3}}))$
A_w	m^2	$A_w = 2*A_{SEh} + \pi*h*L_V$
I_{req} (without coating or lining), A		$I_{req} = i*A_w$
A_{sa}	m^2	$A_{sa} =4\pi*(\frac{d_{sa}}{2})^2$
R_{sa}	Ω	$R_{sa}=\frac{0.315*rho}{\sqrt{A_{sa}*10000}}$
I_{sa}	A	$I_{sa}=\frac{V_{pol-V_p}}{R_{SA}}$
N_1,		$N1=\frac{I_{req}}{I_{sa}}$
Eff %		$\text{Eff }\%=\frac{Ca_{act}}{Ca_{theo}}*100$
W_t,	Kg	$W_t=\frac{C_r*l_d*I_{req}}{eff.*u_f}$
N_2,		$N_2=\frac{W_t}{W_a}$
$I_{req\ (lining\ surface)}$,	A	$I_{req}= i*A_w*F_{bd}$

Open Access
Vol. 14, No. 4, December 2024, pp. 111-128
P- ISSN: 2220-5381
E- ISSN: 2710-1096

1.5 Anode passivation:

It is a phenomenon where sacrificial anodes, designed to protect metal structures from corrosion, lose their effectiveness due to the development of an insulating layer (consists of various substances such as oxides (zinc oxide (ZnO) or aluminum oxide (Al_2O_3)), Mineral Deposit**s** (calcium carbonate ($CaCO_3$) or magnesium hydroxide ($Mg(OH)_2$), Biofouling (marine organisms (barnacles or algae)) on their surface. This layer interferes with the anodes' ability to supply the required electrical current to the protected structure. Passivation can happen in different environments and results from various factors (High Anode Consumption (deplete faster than expected), inadequate Maintenance**:** Neglecting the regular inspection and replacement of sacrificial anodes).

Regular maintenance and cleaning of anodes (removal or reduction of insulating layers using both physical and chemical methods) are crucial to avoid passivation. Moreover, controlling anode consumption by correctly sizing anodes and adhering to replacement schedules can significantly reduce the chances of passivation [11] [10] [12].

1.6 Description of case study problem:

In recent times, dehydrator and desalter at Qubbat Baba Gas Isolation Station has been experiencing corrosion issues, despite the presence of SACP (4 GaIII anodes for each separator). Some of these anodes suffer from a rapid consumption rate in dehydrator, while others suffer from deposits formation, as is the case in desalter as shown in Figure (1). This leads to frequent maintenance and replacement of these anodes in a relatively short period, less than the design life of 5 years, necessitating a study of the causes of this problem and how to address it. Table (2) illustrates Mechanical properties and operating conditions for dehydrator & desalter. Table (3) demonstrates the specifications of metal for dehydrator & desalter. Table (4) explains GaIII specifications.

Journal of Petroleum Research and Studies

Open Access
Vol. 14, No. 4, December 2024, pp. 111-128

P- ISSN: 2220-5381
E- ISSN: 2710-1096

Table (2): Mechanical properties and operating conditions for dehydrator & desalter

Mechanical design		Process design	
Type	Horizontal	Operating pressure, psig	112
Diameter	3.048 m	Operating Temperature, °C	60
Length	12.56 m	Liquid flow, Kg/h	19893
Design Pressure	200 psi	Specific gravity	0.84
Design Temperature,	79 °C	**Material specifications**	
Corrosion allowance,	3.2 mm	Shell	SA-516-70N
Construction code	ASME SEC V.III DIV.1 A97	Head, semi ellipsoidal (2:1)	=
Internal Coating	No Coating	Nozzles Necks	SA-106-B
Internals	**Materials**	Flanges	SA-105N
Inlet Distributers	SA-106 -B (Seamless carbon steel)	Blinds	=
Grids	Carbon Steel	Couplings	=
Sacrificial Anodes	Galvalume III	Studs	SA-193B7
		Nuts	SA-194-2H
		Gaskets	Spiral wound non ASB. Filled 304 stainless steel
		Skirt / Saddle	Saddle

Table (3): Specifications of metal of dehydrator and desalter.

Grade	C%	Si%	Mn%	P%	S%
SA-516-70	0.27-0.31	0.13-0.45	0.79-1.3	0.035	0.035
Properties					
Type	**Tensile strength,**	**Yield strength,**	**Ductility (elongation in 50 mm)**		**Application**
Low carbon steel	485 MPa	260 MPa	21%		Low T&P vessels

Open Access
Vol. 14, No. 4, December 2024, pp. 111-128
P- ISSN: 2220-5381
E- ISSN: 2710-1096

Table (4): Chemical composition and specifications of the GaIII anode alloy

Chemical composition		Properties	
Element	Weight %	Shape	Sphere
Fe	2.554	W_a, Kg	21.3
Zn	1.831	d_{sa}, m	0.249
Carbon	9.2078	Theoretical capacity, A.h/Kg	2971
Tungsten	6.823	Actual capacity, A.h/Kg at 66 C	2690
Aluminum	79.583	Polarized potential, V_p at 66 C	-1.06
The chemical composition of GaIII was analyzed by EDX (Energy Dispersive X-Ray Spectroscopy)-		U_f	0.87
		l_d, year	5
		Consumption rate, C_r, Kg/A.year	3.26
		Eff.%	90.5
		Density, g/cm^3	2.71

Fig. (1): Consumable and deposited GaIII anodes

2. Experimental Work:

All experiments and tests were done in the labs of NOC, PRDC and ministry of technology and science:

2.1 Materials:

Samples were collected from the station include:

- Accumulated corrosion products from the base of dehydrator & desalter.
- Surface Anode deposits.

Open Access
Vol. 14, No. 4, December 2024, pp. 111-128
P- ISSN: 2220-5381
E- ISSN: 2710-1096

- Separated water from dehydrator.
- Separated water from desalter.
- disc coupons of metal of separators SA516-70
- disc coupons of GaIII anode.

2.2 Methods

- **Physical & chemical analysis** for water samples such as (pH, O_2 dissolve, conductivity…etc.) as displayed in Table (5).

Table (5): Physical & chemical analysis for water samples

Property	Desolater Outlet Water	Dehydrator Outlet Water
PH value	6.3	7.2
O_2 Dissolved	10.2	9.63
TDS (ppm)	2875	17740
Calcium (ppm)	150.1	978.5
Magnesium (ppm)	17.1	517.6
Alkalinity (ppm)	244	921
Total Hardness as $CaCO_3$ (ppm)	446.5	4602.8
H_2S (ppm)	742	561
Conductivity @ 25 ° C(ms/cm)	6.8	23.2
Conductivity @ 60 ° C(µs/cm)	8210	2420

- **XRF Analysis:** (x-ray fluorescence technique was used to analyze the corrosion products and the GaIII anode deposits).
- **Potentiostat technique:**

After preparation (polishing, grinding and cleaning) of disc coupons according to ASTM G1 [16]. An electrochemical cell Figure (2) installed which included three electrodes (working electrode(coupon), reference electrode (Ag/AgCl)) and auxiliary electrode Pt/Ti). These electrodes immersed in jacketed vessel included corrosive media (water sample about 600 ml) at 60 º C and then connected to M lab Potentiostat device. Through operating the device, potential, E, and current, i, readings were recorded and plotted in semi log curve (E vs Log i) which is called Tafel curve for anodic and cathodic scan. Based on anodic Tafel slop β_a and cathodic Tafel slop β_c, corrosion potential E_{corr} and corrosion current i_{corr} were concluded. i_{corr} indicated the corrosivity of water and considered a design inputs for SACP system design to calculate the required current for protection I_{req}.

Open Access
Vol. 14, No. 4, December 2024, pp. 111-128
P- ISSN: 2220-5381
E- ISSN: 2710-1096

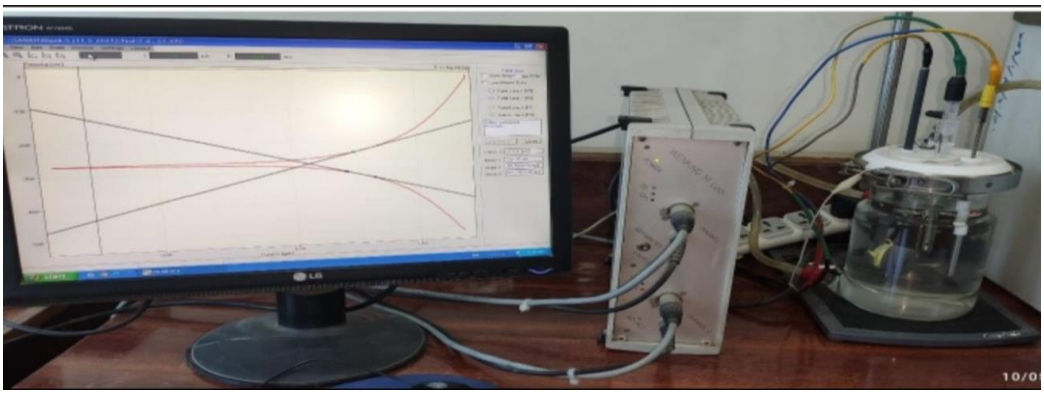

Fig. (2): Potentiostat technique

3. Results and Discussion:

3.1 Potentiostat Results:

Table (6) illustrates corrosion current densities i_{corr} results for SA-516-70 and GaIII coupons in water separated from dehydrator and desalter.

Table (6): Electrochemical results for SA-516-70 and GaIII anode

Sample	$E_{Corr.}$ (mV)	$I_{Corr.}$ ($\mu A/cm^2$)	$\beta_{Cathodic}$ (mV/Dec.)	β_{Anodic} (mV/Dec.)
Dehydrator SA-516-70	-726	10.7	-112.2	48.0
Desalter SA-516-70	-631	40.49	-117	50.6
Dehydrator (GaIII)	-1027	47.98	-138.1	121.8
Desalter (GaIII)	-1022	19.67	-106.9	67.1

From Table (6) and for SA-516-70 coupon, it was observed that the water separated from desalter was more corrosive (about 4 times) than the water separated from dehydrator. While for GaIII anode the opposite appeared.

3.2 XRF Results:

Figures (3) to (5) demonstrates XRF analysis for corrosion products and deposits.

Open Access
Vol. 14, No. 4, December 2024, pp. 111-128

P- ISSN: 2220-5381
E- ISSN: 2710-1096

Z	Symbol	Element	Concentration		Abs. Error	
11	Na2O		< 0.50	%	(0.0)	%
12	MgO		< 0.084	%	(0.0)	%
13	Al2O3		< 0.025	%	(0.0)	%
14	SiO2		< 0.012	%	(0.0)	%
15	P2O5		0.0263	%	0.0031	%
16	SO3		6.400	%	0.009	%
17	Cl	Chlorine	0.01508	%	0.00019	%
19	K2O		< 0.0083	%	(0.0)	%
20	CaO		0.1799	%	0.0046	%
22	TiO2		0.00688	%	0.00070	%
23	V2O5		0.01462	%	0.00062	%
24	Cr2O3		0.2035	%	0.0035	%
25	MnO		0.4824	%	0.0052	%
26	Fe2O3		67.91	%	0.07	%
27	CoO		< 0.0100	%	(0.0)	%
28	NiO		0.1234	%	0.0022	%
29	CuO		0.0636	%	0.0014	%
30	ZnO		0.04308	%	0.00095	%
31	Ga	Gallium	< 0.00042	%	(0.0)	%
32	Ge	Germanium	0.00061	%	0.00026	%
33	As2O3		0.00115	%	0.00032	%
34	Se	Selenium	< 0.00022	%	(0.0)	%
35	Br	Bromine	0.00068	%	0.00013	%
37	Rb2O		0.00060	%	0.00021	%
38	SrO		0.00080	%	0.00015	%
39	Y	Yttrium	0.00122	%	0.00012	%
42	Mo	Molybdenum	< 0.0057	%	(0.0024)	%
47	Ag	Silver	< 0.0011	%	(0.00038)	%
48	Cd	Cadmium	< 0.00086	%	(0.0)	%
50	SnO2		< 0.0024	%	(0.0)	%
51	Sb	Antimony	< 0.0011	%	(0.0)	%
52	Te	Tellurium	< 0.0017	%	(0.0)	%
53	I	Iodine	< 0.0028	%	(0.0)	%
56	BaO	Barium	< 0.0044	%	(0.0)	%
74	WO3		< 0.0031	%	(0.0)	%
80	Hg	Mercury	< 0.00070	%	(0.0)	%
81	Tl	Thallium	< 0.00056	%	(0.0)	%
82	PbO		0.00259	%	0.00082	%
83	Bi	Bismuth	< 0.00045	%	(0.0)	%
90	Th	Thorium	< 0.0091	%	(0.0)	%
92	U	Uranium	< 0.00071	%	(0.0)	%
Sum of concentration			75.47	%		

Fig. (3): XRF analysis for corrosion products from dehydrator

Average Atomic Number:		0.00	Loss of Ignition:		55.6016 %	
Z	Symbol	Element	Concentration		Abs. Error	
11	Na2O		< 0.40	%	(0.0)	%
12	MgO		< 0.069	%	(0.0)	%
13	Al2O3		< 0.021	%	(0.0)	%
14	SiO2		< 0.0089	%	(0.0)	%
15	P2O5		0.0287	%	0.0025	%
16	SO3		4.046	%	0.006	%
17	Cl	Chlorine	0.01381	%	0.00016	%
19	K2O		0.00672	%	0.00049	%
20	CaO		0.2688	%	0.0045	%
22	TiO2		0.0263	%	0.0015	%
23	V2O5		< 0.0024	%	(0.00069)	%
24	Cr2O3		0.0949	%	0.0026	%
25	MnO		0.2796	%	0.0042	%
26	Fe2O3		60.02	%	0.06	%
27	CoO		< 0.0088	%	(0.0074)	%
28	NiO		0.0416	%	0.0015	%
29	CuO		0.0988	%	0.0015	%
30	ZnO		0.1801	%	0.0017	%
31	Ga	Gallium	< 0.00041	%	(0.0)	%
32	Ge	Germanium	< 0.00037	%	(0.0)	%
33	As2O3		0.00139	%	0.00029	%
34	Se	Selenium	< 0.00020	%	(0.0)	%
35	Br	Bromine	< 0.00017	%	(0.00008)	%
37	Rb2O		0.00069	%	0.00018	%
38	SrO		0.00174	%	0.00012	%
39	Y	Yttrium	0.00155	%	0.00011	%
42	Mo	Molybdenum	0.0115	%	0.0046	%
47	Ag	Silver	0.0072	%	0.0010	%
48	Cd	Cadmium	< 0.00085	%	(0.0)	%
50	SnO2		< 0.0016	%	(0.0)	%
51	Sb	Antimony	< 0.0011	%	(0.0)	%
52	Te	Tellurium	< 0.0017	%	(0.0)	%
53	I	Iodine	< 0.0026	%	(0.0)	%
56	BaO	Barium	< 0.0048	%	(0.0)	%
74	WO3		< 0.0036	%	(0.0)	%
80	Hg	Mercury	< 0.00056	%	(0.0)	%
81	Tl	Thallium	< 0.00054	%	(0.0)	%
82	PbO		0.00211	%	0.00070	%
83	Bi	Bismuth	< 0.00043	%	(0.0)	%
90	Th	Thorium	< 0.00078	%	(0.0)	%
92	U	Uranium	< 0.00062	%	(0.0)	%
Sum of concentration			65.13	%		

Fig. (4): XRF analysis for corrosion products from desalter

As it was noticed from the above figures, the ferric oxide Fe_2O_3 was about (60-68)% from corrosion products. Also, SO_3 ratio ranged between 4-6 % revealed the presence of sulfur compounds such as H_2S gas.

Open Access
Vol. 14, No. 4, December 2024, pp. 111-128
P- ISSN: 2220-5381
E- ISSN: 2710-1096

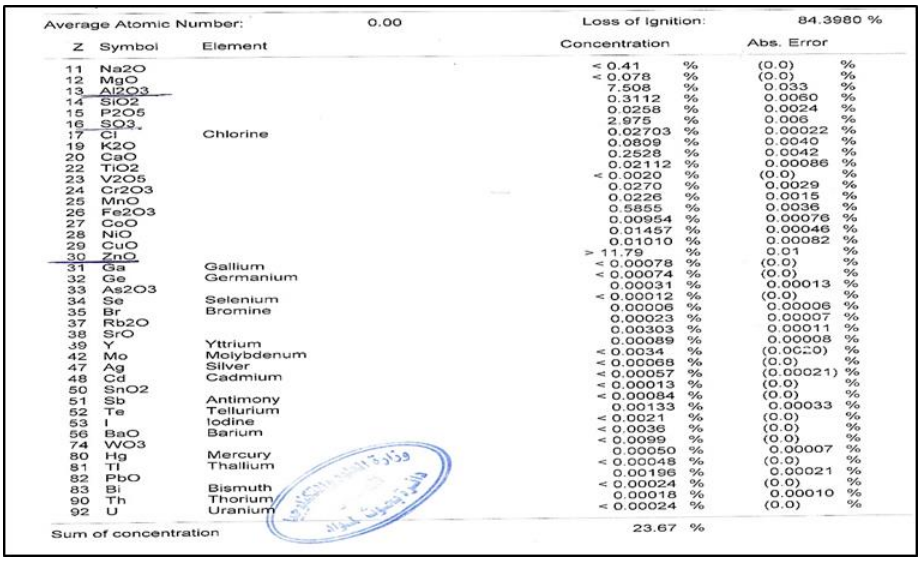

Average Atomic Number: 0.00 Loss of Ignition: 84.3980 %

Z	Symbol	Element	Concentration	Abs. Error
11	Na2O		< 0.41 %	(0.0) %
12	MgO		< 0.078 %	(0.0) %
13	Al2O3		7.508 %	0.033 %
14	SiO2		0.3112 %	0.0060 %
15	P2O5		0.0258 %	0.0024 %
16	SO3		2.975 %	0.006 %
17	Cl	Chlorine	0.02703 %	0.00022 %
19	K2O		0.0809 %	0.0040 %
20	CaO		0.2528 %	0.0042 %
22	TiO2		0.02112 %	0.00086 %
23	V2O5		< 0.0020 %	(0.0) %
24	Cr2O3		0.0270 %	0.0029 %
25	MnO		0.0226 %	0.0015 %
26	Fe2O3		0.5855 %	0.0036 %
27	CoO		0.00954 %	0.00076 %
28	NiO		0.01457 %	0.00046 %
29	CuO		0.01010 %	0.00082 %
30	ZnO		> 11.79 %	0.01 %
31	Ga	Gallium	< 0.00078 %	(0.0) %
32	Ge	Germanium	< 0.00074 %	(0.0) %
33	As2O3		0.00031 %	0.00013 %
34	Se	Selenium	< 0.00012 %	(0.0) %
35	Br	Bromine	0.00006 %	0.00006 %
37	Rb2O		0.00023 %	0.00007 %
38	SrO		0.00303 %	0.00011 %
39	Y	Yttrium	0.00089 %	0.00008 %
42	Mo	Molybdenum	< 0.0034 %	(0.0020) %
47	Ag	Silver	< 0.00068 %	(0.0) %
48	Cd	Cadmium	< 0.00057 %	(0.00021) %
50	SnO2		< 0.00013 %	(0.0) %
51	Sb	Antimony	< 0.00084 %	(0.0) %
52	Te	Tellurium	0.00133 %	0.00033 %
53	I	Iodine	< 0.0021 %	(0.0) %
56	BaO	Barium	< 0.0036 %	(0.0) %
74	WO3		< 0.0099 %	(0.0) %
80	Hg	Mercury	0.00050 %	0.00007 %
81	Tl	Thallium	< 0.00048 %	(0.0) %
82	PbO		0.00196 %	0.00021 %
83	Bi	Bismuth	< 0.00024 %	(0.0) %
90	Th	Thorium	0.00018 %	0.00010 %
92	U	Uranium	< 0.00024 %	(0.0) %
Sum of concentration			23.67 %	

Fig. (5): XRF analysis for GaIII deposits

As it was elucidated from Figure (5), that the XRF results depicted the presence of 7.5% Al_2O_3 and about 12% ZnO which confirmed the occurrence of the passivation phenomenon GaIII anode, hence this corresponds to what is mentioned in Section 1.5.

3.3 SACP Design Results:

According to equations in Table (1), Tables (7) and (8) explain actual SACP design results for dehydrator and desalter respectively.

Table (7): Actual SACP design results for dehydrator

Inputs, units	Outputs , unit	Values
SA-516-70	Area to be Protected A (m^2)	74.8
Bare steel	Current Required (bare), I_{req} (A)	8.004
rho=413 Ω.cm	Number of Anodes based on design life=1year	4
i=0.107 A/m^2	Total Anodes Weight, W_t (kg)	75.41
(Potentiostat results)	Single Anode Resistance, Ra (Ω)	2.948

Table (8): Actual SACP design results for desalter

Inputs, units	Outputs , unit	Values
SA-516-70	Area to be Protected A (m2)	74.8
Bare steel	Current Required (bare), Ireq (A)	30.29
rho=121.8 Ω.cm	Number of Anodes based on design life=1/2year	7
i=0.4049 A/m^2	Total Anodes Weight, Wt (kg)	142.7
(Potentiostat result)	Single Anode Resistance, Ra (Ω)	0.8695

As it was noticed in the above tables, the number of anodes in dehydrator was 4 for 1-year design live instead of 5 years and this predict why anodes consumed quickly. Whlile for desalter,

Open Access
Vol. 14, No. 4, December 2024, pp. 111-128
P- ISSN: 2220-5381
E- ISSN: 2710-1096

the number of anodes was 7 for 6 months' design life only instead of 5 years and this didn't match with the currently installed SACP system. So, for these reasons, a new design for SACP system was proposed to suit the actual conditions for each separator as demonstrated in Tables (9) and (10).

Table (9): A new proposed SACP design for dehydrator

Inputs, units	Outputs, unit	Value
coated steel	Area to be Protected A (m^2)	74.8
with phenolic epoxy	Current Required (coated), $I_r$eq (A)	1.601
bdf=0.2	Number of Anodes based on design life=5 year	4
rho=413 Ω.cm	Total Anodes Weight, W_t (kg)	75.41
i=0.107 A/m^2	Single Anode Resistance, Ra (Ω)	2.948
(Potentiostat results)		

Table (10): A new proposed SACP design for desalter

Inputs, units	Outputs, unit	Value
coated steel	Area to be Protected A (m^2)	74.8
with phenolic epoxy	Current Required (bare), I_{req} (A)	6.058
bdf=0.2	Number of Anodes based on design life=2year	6
rho=121.8 Ω.cm	Total Anodes Weight, W_t (kg)	114.1
i=0.4049 A/m^2	Single Anode Resistance, Ra (Ω)	0.8695
(Potentiostat results)		

The new design proposed phenolic epoxy coating for metal of separators with bdf=0.2. The results explained that dehydrator needs 4 anodes for 5 years to protect coated steel, while desalter needs 6 anodes for 2 years' design life.

4.3 Matlab simulation results for SACP design:

Matlab Simulink is a comprehensive and versatile simulation and modeling platform that enables engineers and researchers to design, simulate, and analyze complex systems efficiently [17] [18]. Figure (6) explains block diagram for simulation steps in Matlab. Figures (7, 8, 9, 10) illustrated simulation models for SACP system design for dehydrator and desalter.

Open Access
Vol. 14, No. 4, December 2024, pp. 111-128
P- ISSN: 2220-5381
E- ISSN: 2710-1096

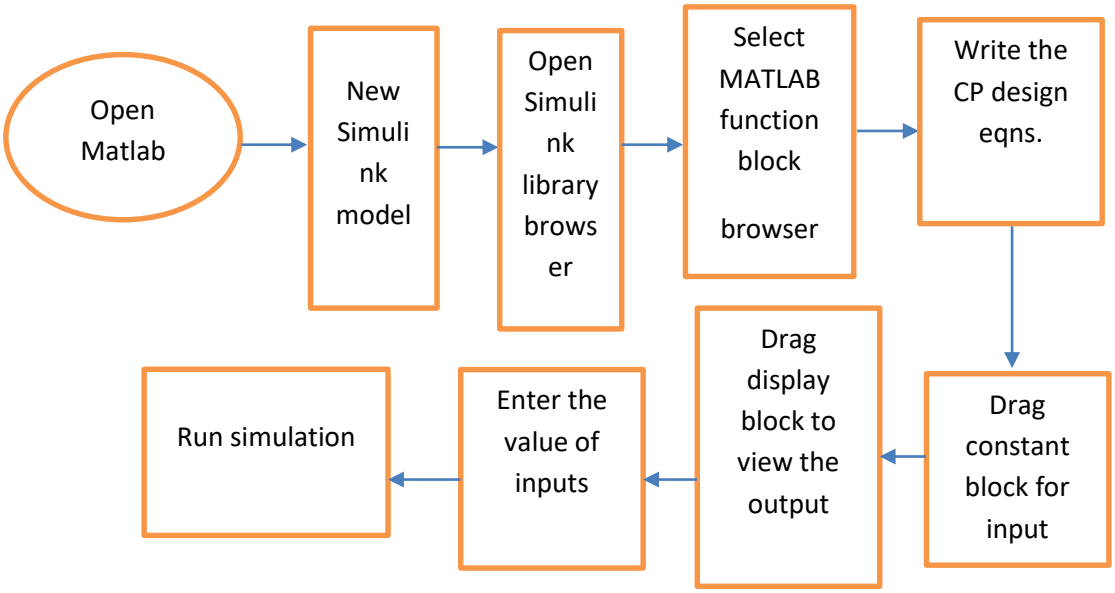

Fig. (6): simulation of CP design steps in Matlab

Fig. (7): Matlab simulation of Actual SACP design for dehydrator

Open Access
Vol. 14, No. 4, December 2024, pp. 111-128

P- ISSN: 2220-5381
E- ISSN: 2710-1096

Fig. (8): Matlab simulation of Actual SACP design for desalter

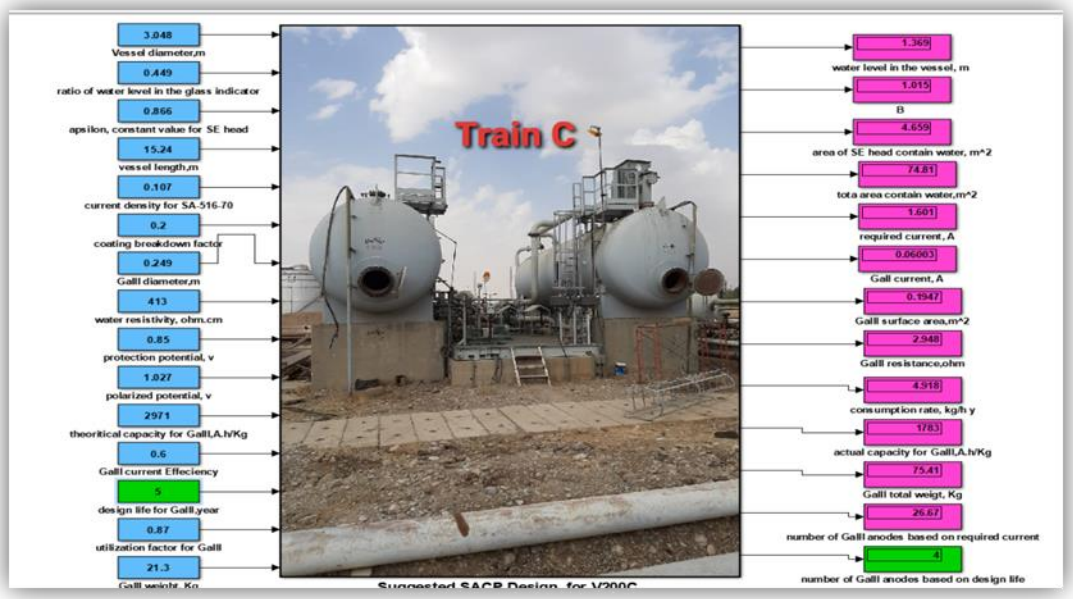

Fig. (9): Matlab simulation of new SACP design for dehydrator

Open Access
Vol. 14, No. 4, December 2024, pp. 111-128

P- ISSN: 2220-5381
E- ISSN: 2710-1096

Fig. (10): Matlab simulation of new SACP design for desalter

From the above figures, we find that simulation has proven its efficiency in performing design calculations. This will assist cathodic protection system design engineers in adapting to potential future alterations in the design parameters.

4. Conclusions

1. Potentiostat results elucidated that separated water from desalter was more corrosive than separated water from dehydrator.
2. XRF analysis proved the formation of oxides on GaIII anode surface includes (Al_2O_3 and ZnO) resulted in passivation of anode which reduces its reactivity and ability to protect metal structure from corrosion.
3. The actual SACP design was not matched with the currently installed system for each separator and desalter.
4. The new proposed design demonstrated that the dehydrator needs 4 anodes for 5 years' design life while desalter needs 6 anodes for 2 years' design life to protect coated steel with phenolic epoxy coating.
5. Matlab simulation proved its efficiency to simulate SACP design with accuracy and flexibility.

Open Access
Vol. 14, No. 4, December 2024, pp. 111-128
P- ISSN: 2220-5381
E- ISSN: 2710-1096

Symbols and Nomenclatures:

Symbol	Meaning or definition	Symbol	Meaning or definition
XRF	X-ray fluorescence	i	Current density
XRD	X-ray diffraction	A_{sa}	Anode area
ZnO	Zinc oxide	R_{sa}	Anode resistance
Al_2O_3	Aluminum oxide	d_{sa}	Anode diameter
h	Water level in dehydrator	rho	Soil resistivity
L_w	ratio of water level (0-1)	I_{sa}	Anode current
D_i	Inside Vessel diameter	N_1, N_2	Number of anodes
A_{SEh}	Area of semi ellipsoidal head	W_a, Wt	Anode weight, total weight of anodes
A_w	Wetted area	F_{bd}	Coating breakdown factor
L_v	Vessel Length	C_r	Consumption rate
l_d	Anode Design life	Eff %,	Anode efficiency
U_f	Utilizing factor	Ca_{theo}, Ca_{act}	Theoretical & actual capacity

Open Access
Vol. 14, No. 4, December 2024, pp. 111-128
P- ISSN: 2220-5381
E- ISSN: 2710-1096

References:

[1] A.W. Al-Mithin, V. Sardesai, H. Sabri and F. Fernando, "sacrificial cathodic protection system inadequacy due to 2 phase operation of 3 phase gas oil separator", in *IPTC 2009: International Petroleum Technology Conference*, Qatar, 2009. https://doi.org/10.3997/2214-4609-pdb.151.iptc14027

[2] J. Pereira, I. Velasquez, R. Blanco, M. Sanchez, C. Pernalete, and C. Canelón, "Crude Oil Desalting Process", *Advances in Petrochemicals*, London, IntechOpen Limited, 2015. https://dx.doi.org/10.5772/61274

[3] M. S. Okyere, "Corrosion Protection for the Oil & Gas Industry", New York: *Taylor & Francis Group*, 2009.

[4] J. L. Hay, "Corrosion Inspection and Control in Refineries", *Shell Projects and Technology, Shell Global Solutions*, Houston, 2013. https://doi.org/10.1520/MNL5820131212917

[5] G. J. P. &. M. D. L. William C. Lyons, "Standard Handbook of Petroleum & Natural Gas Engineering", *Gulf Publishing Company*, Houston, Texas, 2016.

[6] M. Stewart, and K. Arnold, "Gas Liquid and liquid liquid separators", *Gulf professional bublishing*, 2008.

[7] A.W. Peabody, "Peabody's control of pipeline corrosion", *NACE International, The Corrosion Society*, Second Edition 2001.

[8] A. Bhadori, "Cathodic corrosion protection systems: a guide for oil and gas industries", *Elcevier*, 2014.

[9] Headquarters Department of the army Washington, "Electrical design of cathodic protection", *Unified Facilities Criteria (UFC)*, Washington, 2005.

[10] V. Cicek, "Cathodic Protection: Industrial Solutions for Protecting Against Corrosion", *John Wiley & Sons*, 2013.

Open Access
Vol. 14, No. 4, December 2024, pp. 111-128
P- ISSN: 2220-5381
E- ISSN: 2710-1096

[11] R. Winston Revie, "Corrosion and Corrosion Control: An Introduction to Corrosion Science and Engineering", *John Wiley & Sons*, *Elcevier*, 2008.

[12] Z. Ahmad, "Principles of Corrosion Engineering and Corrosion Control", *Butterworth-Heinemann*, *Elcevier*, 2019. https://doi.org 10.1016/B978-0-7506-5924-6.X5000-4

[13] NACE, "System Design Examples for Transmission & other Pipelines", in CP 4- Cathodic Protection Specialist Course Manual, *Nace Internationa*l 2000, pp. 1-70, 2004.

[14] R. C. Doane, "Accurate Wetted Areas for Partially Filled Vessels", *Chemical Engineering*, vol. 114, no. 13, pp. 56-57, 2007.

[15] D. N. Abdulamer, "Effect of soil resistivity on the design of sacrificial anode cathodic protection system", *Journal of Petroleum Research and Studies*, vol. 4, no. 3, pp. 142-158, Dec. 2013. https://doi.org/10.52716/jprs.v4i3.121

[16] ASTM, G1-90, "Standard practice for preparing, cleaning, & evaluating corrosion test specimens", *ASTM International*, 2019.

[17] S. T. Karris, "Introduction to Simulink with engineering applications", *Orchard Publications* , 2006.

[18] S. Eshkabilov, "Beginning Matlab and simulink: From Novice to Professional", *Apress Media LLC*, 2019. https://doi.org/10.1007/978-1-4842-5061-7.